
A Vehicle-Based Laser System for High-Resolution DEM Development – Performance Evaluation of System Components

Peng Li¹, Naiqian Zhang¹, Larry E. Wagner², Fred Fox², Darrell Oard¹,
Hubert Lagae³ and Mingqiang Han¹

¹ Department of Biological and Agriculture Engineering, Kansas State University, Manhattan, Kansas, USA

² USDA-Agricultural Research Service, Fort Collins, Colorado USA

³ USDA-Agricultural Research Service, Manhattan, Kansas USA

Corresponding Author: Naiqian.Zhang@ksu.edu

ABSTRACT

Surface microtopography is quantified by the deviations in the direction of the normal vector of the surface. Soil microtopography is a major factor influencing soil erosion by water and wind. Surface microtopography can be accurately described using the Digital Elevation Model (DEM). In this study, a vehicle-based laser system was developed to generate high-resolution DEM data. The system consisted of five major components: a laser line scanner, a gyroscope sensor, a real-time kinematic GPS, a frame-rail mechanism, and a data acquisition and control unit.

A series of experiments were conducted in the laboratory to evaluate the performance of the components. The result of distance measurements indicated that the system gave the most consistent distance measurement on a white paper. Static gyroscope sensor accuracy tests showed that angle measurement errors observed in combined pitch/roll rotations were larger than in single rotations. Within $\pm 30^\circ$ of single rotations, the measurement errors for pitch and roll angles were within 0.8° and 0.4° , respectively. The tests of the angular displacement on the linear rail showed that it slightly tilted towards the laser line scanner when it moved along the rail.

RÉSUMÉ

La microtopographie de la surface est quantifiée par les déviations dans la direction du vecteur normal de la surface. La microtopographie du sol est un facteur majeur qui influence l'érosion du sol par l'eau et le vent. La microtopographie de surface peut être décrite avec précision en utilisant le modèle numérique d'élévation [Digital Elevation Model (DEM)]. Dans cette étude, un système laser sur véhicule a été élaboré pour générer des données DEM à haute résolution. Le système se compose de cinq éléments principaux : un dispositif de balayage à ligne laser, un capteur gyroscopique, un GPS cinématique en temps réel, un mécanisme cadre-rail et une unité d'acquisition des données et de contrôle.

Une série d'expériences a été menée en laboratoire pour évaluer les performances des composantes. Le résultat des mesures de distance a indiqué que le système a donné la mesure de distance la plus uniforme sur un papier blanc. Les tests de précision du capteur gyroscopique statique ont montré que les erreurs de mesure d'angle observées dans les rotations combinées de tangage/roulis étaient plus importantes que celles des rotations simples. À $\pm 30^\circ$ des rotations simples, les erreurs de mesure des angles de tangage et de roulis étaient respectivement de $0,8^\circ$ et $0,4^\circ$. Les tests du déplacement angulaire sur le rail linéaire ont montré que le rail s'inclinait légèrement vers le dispositif de balayage à ligne laser lorsqu'il se déplaçait le long du rail.

KEYWORDS

Micro topography, Digital Elevation Model, Laser Line Scanner, Gyroscope Sensor.

MOTS CLÉS

Microtopographie, modèle numérique d'élévation, dispositif de balayage à ligne laser, capteur gyroscopique.

CITATION

Li, P., N. Zhang, L.E. Wagner, F. Fox, D. Oard, H. Lagae and M. Han. 2021. **A Vehicle-Based Laser System for High-Resolution DEM Development – Performance Evaluation of System Components**. Canadian Biosystems Engineering/Le génie des biosystèmes au Canada 63: 2.23-2.31. <https://doi.org/10.7451/CBE.2021.63.2.23>

INTRODUCTION

Soil microtopography is a crucial factor influencing soil erosion by water and wind (Moreno et al., 2008). Soil erosion is related to soil surface processes, such as infiltration, runoff, gas exchange, sediment transport, and deposition. Surface microtopography is a dynamic soil property that controls these physical processes (Darboux and Huang, 2001). Therefore, studying these processes and their spatial variations requires accurately describing surface microtopography.

As such, it is a critical measurement necessary to comprehensively assess the surface and soil conditions affecting soil erosion, both wind and water-induced, in laboratory and field experiments. The ability to obtain such micro-topography measurements easily and quickly at sufficient or desired accuracy greatly enhances erosion studies. Applying a non-contact or no surface disturbance measurement also provides the ability to measure surface microtopography changes that occur over time due to climatic and other disturbance factors. This is possible by obtaining repeated measurements from the same site multiple times.

Many researchers have studied the mechanisms of these processes. Various techniques to measure surface microtopography were developed over the past years to assist these studies. These techniques can be classified by spatial dimensions and sensor types (Jester and Klik, 2005). To acquire limited surface characterization, two-dimensional measurements used simple tools, such as a pin meter or a roller chain. Three-dimensional measurements gave a more realistic surface representation and allowed more analysis of surface parameters. Concerning the sensor type, measurement techniques can be divided into contact and non-contact types. The contact type disturbed the soil surface with pins, or a chain set for height measurement, whereas the non-contact type measured the distance from the soil surface to a reference plane without touching the soil surface (Robichaud and Molnau, 1990). The non-contact type allowed monitoring of changes in soil microtopography over time. Sensors used for these methods fell into four categories: infrared, ultrasonic, photogrammetry, and laser.

The pin method was the dominant technique for measuring soil microtopography before the 1990s. A pin meter consisted of a single pin or a row (or even multiple rows) of evenly spaced pins. When measuring the elevation, the pins were lowered manually or automatically onto the soil surface until contact between the pins and the soil surface was made. Surface elevations were then registered manually, electronically, or photographically from the relative heights of the pins and later digitized (Podmore and Huggins, 1981; Radke et al., 1981; Wagner and Yu, 1991). The roller chain was another contact method for measuring soil microtopography. This method used chain-like devices placed across a surface. Soil microtopography was mechanically measured by calculating the horizontal length reduction of the chain (Saleh, 1993; Merrill et al., 2001).

The pin and chain methods were simple, inexpensive techniques. However, being a contact-type measurement, these methods disturbed and damaged the original soil surface profile, especially on loose or wet soils. Furthermore, a significant deficiency of the roller chain type of micro topography measurement is that several different scales of micro topography could give the same or similar value. For example, a ridged elevation of 1" height with a spacing of 2" and another ridge elevation of 2" height with a spacing 1" would be very similar but, in essence, were very different surfaces (Skidmore, 1997).

An early non-contact technique to measure soil microtopography used an infrared profiler meter (Romkens and Wang, (1986). The meter included an infrared probe which detected the soil surface in predetermined transects. The horizontal and vertical movement of the probe was controlled by DC electric motors. Encoders recorded the position of the probe. The profiler frame was mounted on utility vehicles to allow measurements of different transects. The covered area was 1 m by 1.15 m. A vertical accuracy of 3mm was reported. However, due to the difference in reflectivity of different surfaces, the profiler meter was only used on surfaces with a uniform albedo.

Ultrasonic technology was widely used in distance measurement. Ultrasonic waves in distance measurement were called SONAR (sound navigation and ranging). A non-contact ultrasonic profiler was developed by Robichaud and Molnau (1990) to measure soil microtopography. This profiler used an ultrasonic transducer to emit an ultrasonic wave to the soil surface and then received the reflected signal. The time between transmission and reception of the signal was proportional to the distance between the sensor and the soil surface. A 1.5 m by 1.5 m aluminum frame was used as the base to provide a reference plane. A stepper motor controlled the movement of the ultrasonic sensor on the frame. This profiler achieved a vertical accuracy of 3 mm and a horizontal resolution of 30 mm.

Photogrammetry was the first remote sensing technology developed to determine the geometric properties of objects from photographic images (WFI, 2009). A more sophisticated technique, called stereophotogrammetry, could estimate the three-dimensional coordinates of points on an object. These coordinates were measured in two or more photographic images taken from different positions and angles with common reference points in each image (Welch et al., 1984; Warner, 1995; Taconet and Ciarletti, 2007; Cierniewski et al., 2015; Gilliot et al., 2017). The photogrammetric technique could reduce the data acquisition time for images covering large areas. However, interpretations of the photogrammetric data were complicated (Jester and Klik, 2005).

Lasers have been widely used in range measurement due to their ability to obtain more accurate measurements than most alternative methods. Most laser rangefinders project a visible or infrared laser beam onto a target to which the distance was to be measured. A light detector then receives the beam reflected from the target. The distance between the

target and the laser sensor was determined based on the triangulation principle, which calculated the distance by knowing where the reflected beam fell on the detector. The laser systems for automated, non-contact measurements of surface elevation commonly include three major components: a) a laser transducer with a receiver to detect the distance; b) a computer-controlled, motor-driven, two-dimensional traversing frame; and c) a PC with a set of interface circuitry to control the motion of the laser carriage and to register the elevation data (Bertuzzi et al., 1990; Huang and Bradford, 1990; Flanagan et al., 1995; Wilson et al., 2001; Darboux and Huang, 2003; Lichti and Jamtsho, 2006). The laser method was not very convenient for frequent field experiments because it required transporting a heavy traversing frame. In contrast, the calibration of the device is complicated, and data processing requires the use of expert software and extensive knowledge of image processing (Mizaei et al., 2012; Bretar et al., 2013; Thomsen et al., 2015). Moreover, hidden objects in the reflection path could cause missing data.

Each of these methods had advantages and disadvantages. For field studies and applications, the system used to measure soil microtopography should be portable, accurate, and not computation intensive. Hence, the overall objective of this research was to develop a real-time, field-portable, vehicle-based laser measurement system capable of measuring geo-referenced surface elevations at a sub-inch accuracy and a sufficient horizontal resolution. Portability was accomplished by mounting a linear rail frame supporting a laser system on a 4x4 vehicle. A high horizontal resolution was achieved using a high-speed interface PCI card for the laser system with a high data acquisition speed. With little manual effort, the PC and software reached the desired level of automation to produce DEMs and other surface roughness indices quickly.

As the first of a two-paper series, this paper focuses on the system components' design, construction, and performance tests. For micro-topography measurement on various types of surfaces, several factors may affect the measurement accuracy: (1) the consistency in distance measurement of the laser line-scanner on surfaces with different reflection properties, (2) varying slopes of the surface where the vehicle is parking or moving on, and (3) deformation of the supporting rail when the laser sensor moves along the rail.

Thus, the specific objectives of the work reported in this paper are: (1) to provide a detailed description of the system design, (2) to examine the consistency of the laser scanner in distance measurement on different types of surfaces, (3) to examine the effectiveness of the gyroscope sensor in measuring and compensating for the surface slope on DEM measurement, and (4) to examine the measurement error caused by deformation of the rail.

The developed system was tested in DEM measurement under laboratory and field conditions. The test procedures and results will be reported in the second paper of the two-paper series.

MATERIALS AND METHODS

The design of the vehicle-based DEM measurement system is described below, followed by experimental procedures and statistical analyses for the testing of three key components – laser distance sensor, gyroscope sensor, and linear rail.

System Design and Construction

The vehicle-based laser measurement system developed in this study consisted of five major components: 1) a distance-measuring unit, 2) a frame-rail unit, 3) a frame angular-position measuring unit, 4) a geo-referencing unit, and 5) a data-acquisition and control unit.

Distance-measuring Unit: Laser Line Scanner An AccuRange Line Scanner, AccuRange 4000-LIR (Acuity Research Inc., 2000), was used to measure the surface elevation. This scanner consisted of an elliptical, rotating mirror driven by a DC motor with an optical encoder and mounting hardware for use with Acuity's 4000 laser rangefinder. The measurement principle of the laser line scanner is demonstrated in Fig. 1. A laser diode emitted a collimated infrared laser beam of 780 nm wavelength. The beam was deflected 90 degrees toward the target by the rotating mirror. The target reflected the laser beam to the sensor through the same mirror. By knowing the travelling time of the laser beam, the distance between the sensor and the target can be determined. The elliptical mirror was situated at a 45-degree angle from the incident laser beam and was rotated continuously by a DC motor. The mirror was engineered to reflect 96% of the incident light. An optical encoder with 4096 counts per revolution was attached to the motor to record the mirror's angular position. The laser line scanner measured distances of up to 15.24 m with a 2.54 mm accuracy.

Vehicle-based Frame-rail Supporting Unit: An ER belt-driven linear rail with 2m working length (Parker Hannifin Corp., 2004), as shown in Fig. 2, was selected to move the

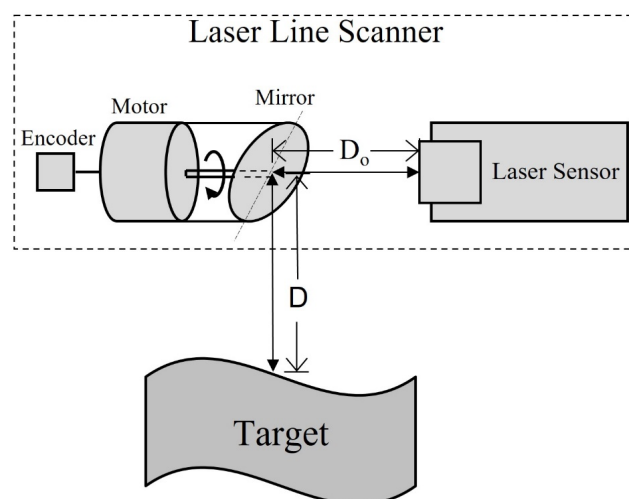


Fig. 1. Measurement principle of the laser line scanner.

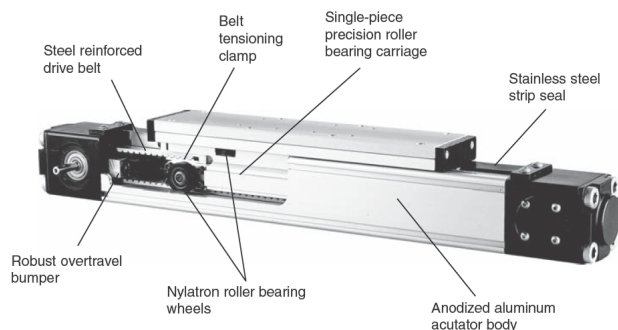


Fig. 2. The linear rail (Parker Hannifin Corp., 2004).

laser line scanner in the direction perpendicular to its scan plane for surface measurement. A 12V DC geared motor was mounted at one end of the rail to control the translational motion of the laser scanner. An incremental optical encoder with 200 pulses per rotation (BEI Industrial Encoders, model H20) was attached to the motor to provide feedback signals on the position of the laser scanner.

An aluminum frame was designed to support the rail (Fig. 3). This frame had a sliding structure that allowed two sliding arms to extend for up to 1 meter. The sliding arms could also be raised for more than 1m with the help of the slotted arcs. By adjusting the length and height of the sliding arms, the scanning width can be adjusted from 1m to 2 m. A 1/4-inch-thick flat plate was mounted on two small slide arcs at the end of the sliding arms. The linear rail was mounted on a flat plate with four toe clamps. Thus, the level of the linear rail can be adjusted. The rectangular base of the frame could easily fit into the bed of a small utility vehicle.

Frame Angular-position Measuring Unit: Gyroscope Sensor A gyroscope sensor, AHRS400CD-100 Motion and Attitude Sensing Unit (Crossbow Technology Inc., 2005), was selected to measure the roll, pitch, and yaw angular displacements of the frame under static and dynamic conditions. The gyroscope sensor was a nine-axis measurement system that integrated linear accelerometers, rotational rate sensors, and magnetometers. It used a 3-axis accelerometer and 3-axis rate sensor to accomplish complete measurements of the system dynamics. Adding a 3-axis magnetometer also allowed the sensor to measure magnetic heading accurately.

Geo-referencing Unit: RTK GPS The geo-reference unit was used to provide the global position information of the measured surface and to convert the measurement results from a local coordinate system to the global coordinate system. A Real-time Kinematic (RTK) GPS, Topcon HiPer Lite+ (Topcon Positioning System Inc., 2006), was used to help register the measured surface into a geographic coordinate system. The System consisted of a HiPer Lite+ Base, a standard HiPer Lite+ Rover, and an FC-100 data collector with TopSURV data collection software. It gave static accuracies of 3 mm horizontal and 5 mm vertical. The kinematic accuracies were 10 mm horizontal and 15 mm vertical.

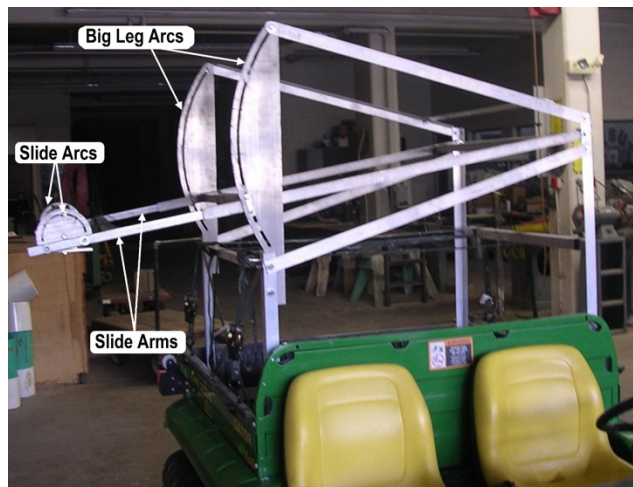


Fig. 3. The aluminum frame that allowed adjustment of the scan area.

Data acquisition and Control Unit: The laser line scanner was configured with a High-Speed Interface (HSIF) PCI card (Schmitt Measurement Systems Inc., 2005) to increase the sample rate. The HSIF card had two pulse-width modulated motor control channels, two 32-bit quadrature decoders to read motor encoders, and three general-purpose inputs. A motor control channel with a quadrature decoder was used to monitor the angular displacement of the rotating mirror. Another motor channel and quadrature decoder were wired to the DC motor on the linear rail. The gyroscope sensor and the Rover of RTK GPS were configured as standard serial interfaces. A ruggedized field laptop computer (GETAC Inc., model GETAC A770) was used to acquire data from different components. Figure 4 displays the connections among the system components. The utility vehicle's 12V battery powered the entire system.

A user interface program was developed in C to control the laser system and acquire the sensor data through the field laptop. There were three raw data files created. One was for sequential laser samples. Another was for a sequence of the gyroscope data packets. The last one logged the location data from the GPS.

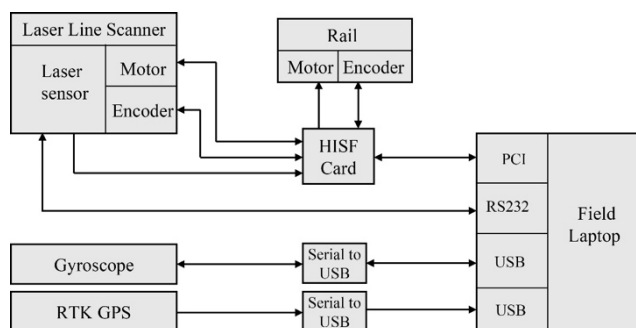


Fig. 4. The data acquisition and control system.

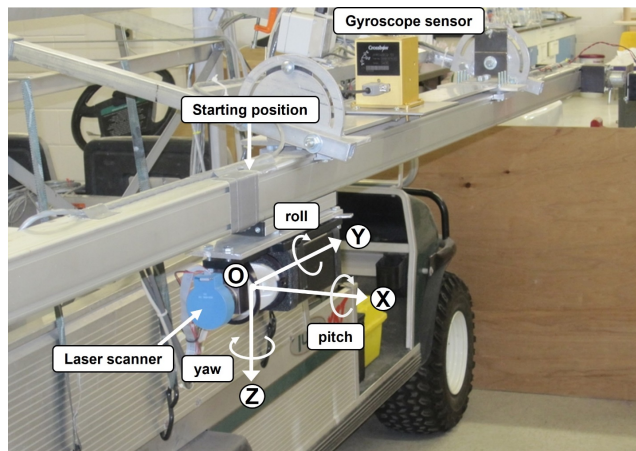


Fig. 5. The local coordinate system.

System Components Tests – Experiment Procedure

Distance Measurement The reflective characteristic of the target material was an important factor affecting distance measurement accuracy. In the laboratory, a test was conducted to evaluate the performance of the laser line scanner on different target objects and to calibrate the distance measurement. The target objects tested were white paper, black paper, and sand. During the test, the target object was positioned at seven different distances from the center of the rotating mirror. The laser sensor took distance measurements at each position for 15-18 seconds. An average number of 80,000 measurements were taken for each distance, and the standard deviations of the measurement errors at each distance were compared among the three surfaces.

Static Accuracy Test for the Gyroscope Sensor The attitude of the linear rail, measured by the gyroscope sensor, was used to correct the elevation data. For this purpose, the gyroscope sensor should provide reliable and accurate angle measurements, especially for the roll and pitch angles. A test was conducted to examine the measurement errors of the gyroscope sensor in measuring pitch, roll, and combined pitch/roll rotations. A milling machine (Enco Manufacturing Co.) was used as a two-dimensional testing platform. With the gyroscope sensor fastened on the drill head, the machine can provide two-axis rotations to the gyroscope sensor. During the static test, the gyroscope was tested with pitch rotation only, roll rotation only, and combined pitch and roll rotations. Pitch and roll rotations of up to $\pm 45^\circ$ with a 1° increment were tested to simulate the gyroscope sensor on the laser system. At each angle, the average value of 4,000 measurements was compared with the actual angle read from the dials of the milling machine. The absolute error was calculated between the average measurement value and the actual angle. The maximum absolute error is used to evaluate the sensor.

Angular Displacement of the Linear Rail The local coordinate system of the laser system (Fig. 5) was defined on the laser scanner, which was mounted on the linear rail.

If there were changes in the roll and pitch angles of the rail during scanning, the coordinates of the measured surface ground would change. The rail was mounted on the ends of two sliding arms (Figure 3) but not supported against the ground at any point. When the laser carriage moved along the rail, the pitch and roll angles of the rail would unavoidably vary due to the weight of the laser carriage, causing small rotations of the coordinate system, hence measurement errors.

Thus, a test was conducted to investigate the changes in the roll and pitch angles of the linear rail when the laser carriage moved along the rail. The test was conducted under two conditions for comparison: 1) the rail was supported at the two ends against the ground, and 2) the rail was not supported. The gyroscope sensor measured the roll and pitch angles at combinations of three speeds of the laser carriage movement (6.31cm/s, 9.32cm/s, and 14.63cm/s) and three speeds of the laser mirror rotation (1400 RPM, 2000 RPM, and 2600 RPM). The "starting" position of the laser carriage was 66 cm from the front end of the rail. The "ending" position was 120 cm away from the starting position. The angular displacement of the linear rail was evaluated by the ranges of variation of the roll and pitch angles as measured by the gyroscope sensor when the laser carriage moved from the starting to the ending positions.

RESULTS AND DISCUSSION

Distance Measurement

The standard deviations of measurement errors of approximately 80,000 measurements obtained at each distance from the three target objects are plotted in Fig. 6. The distance measured from the white and black papers had the least and most errors, respectively, whereas the measurement error from the sand surface was in between. This was probably because the black paper absorbed the laser light most, resulting in the weakest reflection. The white paper had the smallest absorption and hence the strongest reflection among the three types of surfaces. Based on these results, the white paper was selected as the target object to calibrate the distance measurement.

Static Accuracy Test for the Gyroscope Sensor

The pitch and roll angle measurement errors obtained in the milling machine are shown in Fig. 7. For both pitch and roll angles, the measurement errors generally increased as the actual pitch and roll angles increased. Within the $\pm 30^\circ$ range, the maximum absolute errors of pitch and roll angle measurements were about 0.80° and 0.40° , respectively.

Figure 8 showed the absolute errors for the pitch and roll angles when both pitch and roll rotations existed in four cases: (1) positive pitch and roll, (2) negative pitch and roll, (3) positive pitch with negative roll, and (4) negative pitch with a positive roll. From the results, it can be concluded that when the pitch or roll angle varied within $\pm 30^\circ$, the absolute measurement errors for both pitch and roll angles were maintained within 1° , except for the positive roll and negative pitch combination, where the maximum absolute measurement error for roll angle reached near 2° .

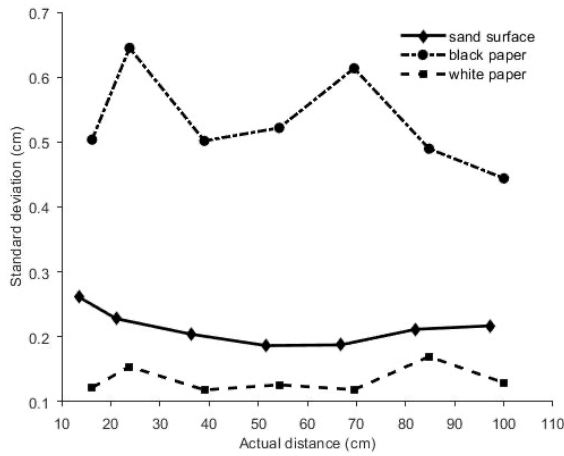


Fig. 6. Standard deviations of distance measurements from three target objects.

Angular Displacement of the Linear Rail

Roll angles measured by the gyroscope sensor under two different conditions - when the rail was not supported at the ends and when it was supported - are plotted in Fig. 9. The results showed that roll angles under both conditions had small variations when the laser carriage moved along the rail. All the measured roll angles were maintained within the range of 0.16° , which would cause a positioning error of less than ± 1.4 mm on the ground in the lateral direction if the laser scanner was mounted 1 m above the ground.

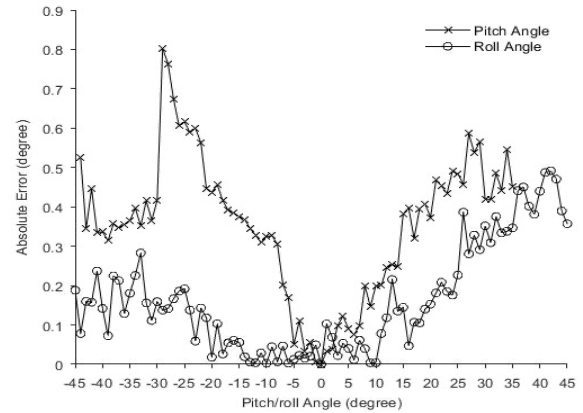


Fig. 7. Absolute pitch and roll measurement errors were observed in single pitch/roll rotations.

Pitch angles measured by the gyroscope sensor when the linear rail was and was not supported at the two ends are plotted in Fig. 10. It is obvious that when the linear rail was not supported, the pitch angle gradually decreased when the laser carriage moved from the starting position toward the ending position. The range of the pitch angle variation was about 0.4° , which would cause a positioning error of less than ± 7 mm on the ground in the longitudinal direction if the laser scanner was mounted 1 m from the ground.

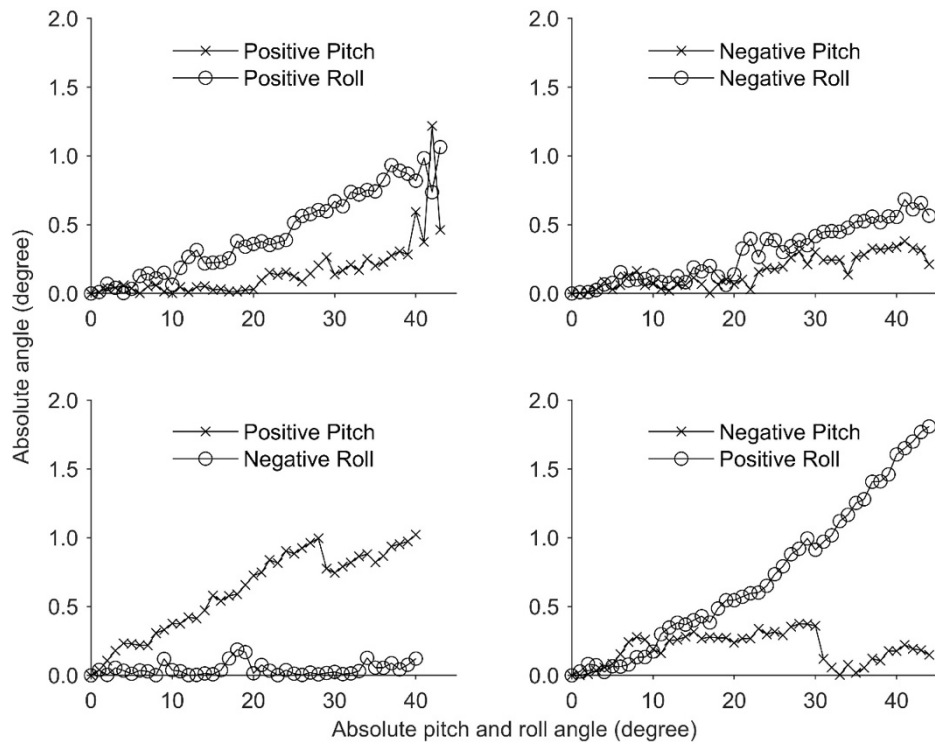


Fig. 8. Absolute errors for pitch and roll measurement observed in four cases: (a) positive pitch and roll, (b) negative pitch and roll, (c) positive pitch and negative roll, and (d) negative pitch and positive roll.

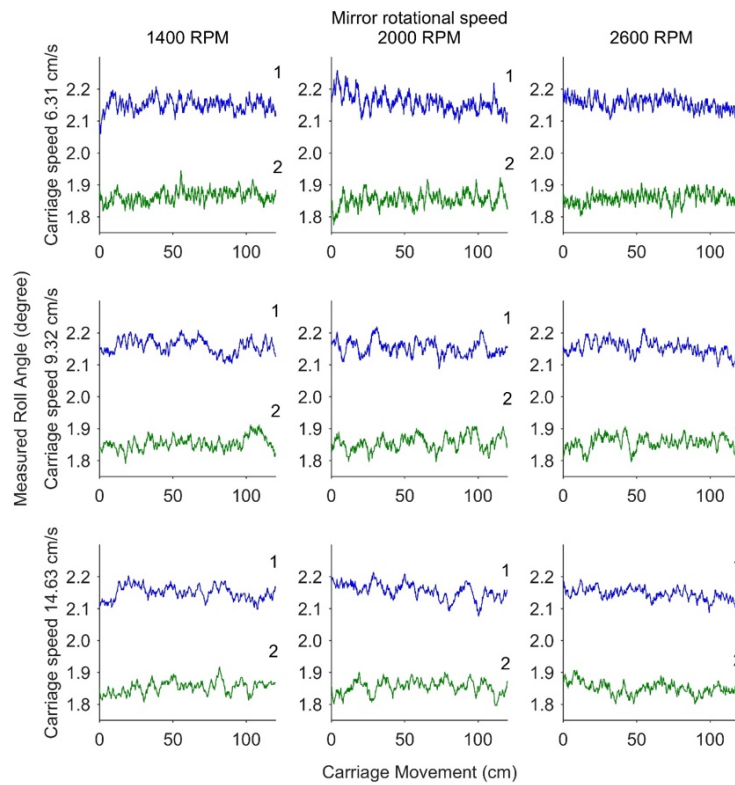


Fig. 9. Roll angles measured by the gyroscope sensor under two conditions: (1) when the rail was not supported (blue) and (2) when the rail was supported (green).

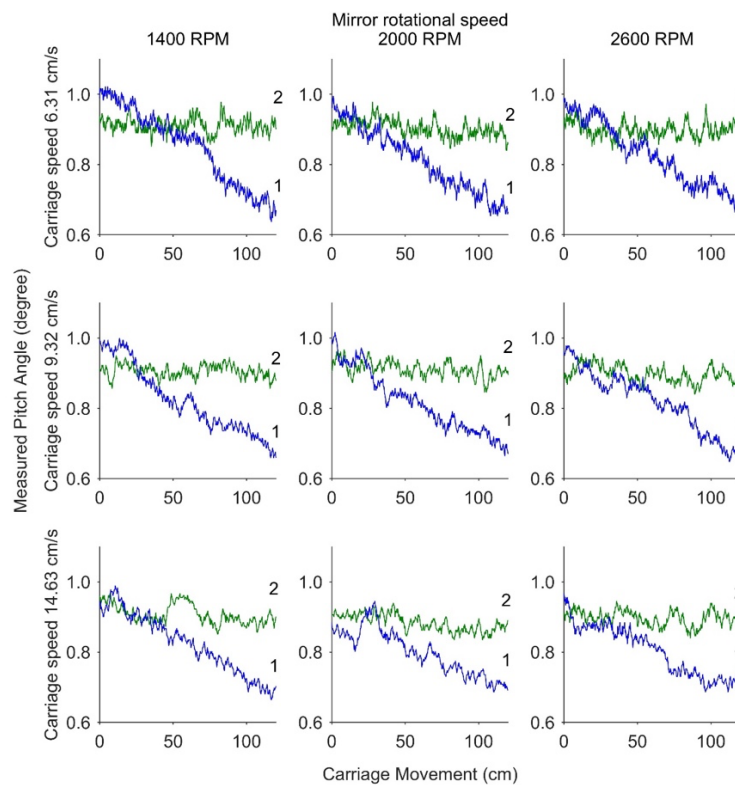


Fig. 10. Pitch angles measured by the gyroscope sensor under two conditions: (1) when the rail was not supported (blue) and (2) when the rail was supported (green).

This trend was not found when the rail was supported at two ends. Thus, it can be concluded that the rigidity of the aluminum frame that supported the rail was not sufficient. The rail slightly tilted towards the direction where the laser line scanner moved because of the change in weight balance on the rail.

Portability and Measurement Resolution

As previously discussed, the existing micro-topography measuring techniques, including the contact type (pin and roller chain) and non-contact type (infrared, ultrasonic, photogrammetry, or laser), were all designed for measuring surface topography within a fixed area, which is either a physical frame to mount multiple sensors (pins or roller chains), a fixed frame to mount a travelling sensor (laser), or a fixed position to mount a sensor that scans through a fixed area (infrared, ultrasonic, or photogrammetry). Thus, the measurements these devices obtained were elevation changes relative to the fixed sensor frame or sensor position but not the absolute elevation relative to a common reference, such as the sea level. As a result, none of these techniques were "portable." The vehicle-based laser system reported in this paper, on the other hand, used an RTK-GPS to provide the accurate position of the sensor in the global coordinate system and a gyro sensor to provide pitch, roll, and yaw angles of the sensor to correct for elevation measurement errors in a 3D space, thus producing real DEM data. The test results of the static and dynamic measurement errors caused by the gyro sensor and the rail deformation indicated that the system can be used at different locations with different surface slopes and still provide absolute elevation measurement.

Being a vehicle-based, portable system, the DEM measurement can be accomplished in two modes: (1) dynamic mode, where the measurement is conducted continuously when the vehicle keeps travelling at a slow speed and (2) static mode, where the vehicle stops intermittently, and the measurement is done at each stop. For the static mode, three factors determine the measurement resolution – (1) the speed at which the carriage moves along the linear rail, (2) the rotational speed of the mirror in the laser sensor, and (3) the throughput of the data acquisition system. During the tests, the highest mirror rotational and carriage speeds were 2,600 RPM and 14.63 cm/s (0.327 mph), respectively. The laser data are sampled in the high-speed interface at a sampling frequency of 50,000 Hz. At these speeds and with the laser sensor mounted 1 m from the surface, the system can complete measurement of a 1m by 1m area within 6.84 seconds with measurement resolutions in the longitudinal and lateral directions of 0.34 cm and 0.7 cm, respectively. Lower resolutions can be achieved by reducing the mirror rotational speed, the sampling frequency of the high-speed interface, or increasing the carriage speed along the rail. For the dynamic mode, the same resolutions can be achieved when the vehicle moves at the speed of 14.63 cm/s, and the laser sensor remains at the central position without moving on the rail, thus reducing the effect of the angular movement

of the rail on the DEM measurement. A setback of the dynamic mode is potential variations in the attitude of the rail (pitch, roll, and yaw angles) and associated vibrations due to the uneven surface. Thus, for the dynamic mode, dynamic compensations for the attitude variations provided by the gyro sensor become important.

The portability and fine resolution in DEM measurement are the features that separate the vehicle-based laser system reported in this paper from other micro-topography measurement technologies.

CONCLUSIONS

A vehicle-based laser measurement system was developed to measure surface microtopography and generate DEM data. A series of experiments was conducted to evaluate the performance of each component of the system. After testing the laser scanner on three types of target objects – white paper, black paper, and sand, it was found that the white paper gave the most consistent distance measurement with a standard deviation of 0.18 cm within the measurement range of 100 cm. The static test of the gyroscope sensor showed that errors in pitch and roll angle measurement when only roll or pitch rotation existed were smaller than when both pitch and roll rotations existed. Within $\pm 30^\circ$ of single pitch or roll rotations, the measurement errors in pitch and roll angles were within 0.8° and 0.4° , respectively. Within the $\pm 30^\circ$ range of combined rotation, the measurement errors for both pitch and roll angles were within 1° . The test results for angular displacement of the linear rail indicated that the rail always tended to tilt in the direction where the laser scanner was located. These changes were related to the weight balance on the linear rail. However, the roll angles were maintained within 0.16° , with small variations when the laser carriage moved along the rail.

ACKNOWLEDGEMENTS

The authors acknowledge the financial support of the U.S. Department of Agriculture, Agricultural Research Service (Agreement No.58-5430-8-317).

REFERENCES

- Acuity Research Inc. 2000. AccuRange Line Scanner User's Manual. Rev. 2.3. Menlo Park, CA: Acuity Research, Inc.
- Bertuzzi, P., J. Caussignac, P. Stengel, G. Morel, J. Lorendeau, and G. Pelloux. 1990. An automated, non-contact laser profile meter for measuring soil roughness in situ. *Soil Science* 149(3): 169-178.
<https://doi.org/10.1097/00010694-199003000-00006>
- Bretar, F., M. Arab-Sedze, J. Champion, M. Pierrot-Deseilligny, E. Heggy, S. Jacquemoud. 2013. An advanced photogrammetric method to measure surface roughness: Application to volcanic terrains in the Piton de la Fournaise, Reunion Island. *Remote Sensing of Environment* 135: 1-11.
<https://doi.org/10.1016/j.rse.2013.03.026>
- Cierniewski, J., A. Karnieli, C. Kazmierowski, S. Krolewicz, J. Piekarczyk, K. Lewinska, A. Goldberg, R.

- Wesolowski, M. Orzechowski. 2015. Effects of soil surface irregularities on the diurnal variation of soil broadband blue-sky albedo. *IEEE Journal of Selected Topics in Applied Earth Observations and Remote Sensing* 8(2): 493-502.
<https://doi.org/10.1109/JSTARS.2014.2330691>
- Crossbow Technology Inc. 2005. AHRS400 Series User's Manual. Rev. A. San Jose, CA: Crossbow Technology, Inc.
- Darboux, F. and C. H. Huang. 2003. An instantaneous-profile laser scanner to measure soil surface microtopography. *Soil Science Society of America Journal* 67(1): 92-99.
<https://doi.org/10.2136/sssaj2003.9200>
- Darboux, F. and C. H. Huang. 2001. Contrasting effects of surface roughness on erosion and runoff. *Soil Erosion Research for the 21st Century*: 143-146.
- Gilliot, J.M., E. Vaudour, J. Michelin. 2017 Soil surface roughness measurement: A new fully automatic photogrammetric approach applied to agricultural bare fields. *Computers and Electronics in Agriculture*. 134: 63-78. <https://doi.org/10.1016/j.compag.2017.01.010>
- Flanagan, D., C. Huang, L. Norton, and S. Parker. 1995. Laser scanner for erosion plot measurements. *Trans. ASAE* 38(3): 703-710.
<https://doi.org/10.13031/2013.27883>
- Huang, C. and J. M. Bradford. 1990. Portable laser scanner for measuring soil surface roughness. *Soil Science Society of America Journal* 54(5): 1402-1406.
<https://doi.org/10.2136/sssaj1990.03615995005400050032x>
- Jester, W. and A. Klik. 2005. Soil surface roughness measurement - methods, applicability, and surface representation. *Catena* 64(2-3): 174-192.
<https://doi.org/10.1016/j.catena.2005.08.005>
- Lichti, D.D., S. Jamtsho. 2006. Angular resolution of terrestrial laser scanners. *The Photogrammetric Record* 21(114):141-160. <https://doi.org/10.1111/j.1477-9730.2006.00367.x>
- Merrill, S., C. Huang, T. Zobeck, and D. Tanaka. 2001. Use of the chain set for scale-sensitive and erosion-relevant measurement of soil surface roughness. In *Proc. of 10th international soil conservation organization meeting*. 594 - 600.
- Mirzaei, M., S. Ruy, T. Ziarati. 2012. Monitoring of soil roughness caused by rainfall using stereo-photogrammetry. *International Research Journal of Applied and Basic Sciences* 3(2): 322-338
- Moreno, G. R., D.M.C. Alvarez, S.A. Requejo, and A. M. Tarquis. 2008. Multifractal analysis of soil surface roughness. *Vadose Zone Journal* 7(2): 512-520.
<https://doi.org/10.2136/vzj2007.0016>
- Parker Hannifin Corp. 2004. ER Series Rodless Actuators. Wadsworth, OH: Parker Hannifin Corp.
[https://doi.org/10.1016/S1365-6937\(04\)00177-7](https://doi.org/10.1016/S1365-6937(04)00177-7)
- Podmore, T. and L. Huggins. 1981. An automated profile meter for surface roughness measurements [for tillage effectiveness]. *Trans. ASAE* 24(3):663-665,669.
<https://doi.org/10.13031/2013.34317>
- Radke, J., M. Otterby, R. Young, and C. Onstad. 1981. A microprocessor automated rillmeter [Soil erosion]. *Trans. ASAE* 24(2): 401-404,408.
<https://doi.org/10.13031/2013.34264>
- Robichaud, P. and M. Molnau. 1990. Measuring soil roughness changes with an ultrasonic profiler. *Trans. ASAE* 33(6): 1851-1858.
<https://doi.org/10.13031/2013.31549>
- Romkens, M. and J. Wang. 1986. Effect of tillage on surface roughness. *Trans. ASAE* 29(2): 429-433.
<https://doi.org/10.13031/2013.30167>
- Saleh, A. 1993. Soil roughness measurement: chain method. *Journal of soil and water conservation* 48(6): 527-529.
- Schmitt Measurement Systems Inc. 2005. AccuRangTM High Speed Interface PCI Formats User's Manual. Rev. 6.2. Portland, OR: Schmitt Measurement Systems, Inc
- Skidmore, E.L. 1997. Comment on Chain Method for Measuring Soil Roughness. *Soil Science Society of America Journal* 61(5) <https://doi.org/10.2136/sssaj1997.03615995006100050034x>
- Taconet, O. and V. Ciarletti. 2007. Estimating soil roughness indices on a ridge-and-furrow surface using stereo photogrammetry. *Soil tillage research* 93(1): 64-76. <https://doi.org/10.1016/j.still.2006.03.018>
- Thomesen, L.M., J.E.M. Baartman, R.J. Barneveld, T. Starkloff, J. Stolte. 2015. Soil surface roughness: comparing old and new measuring methods and application in a soil erosion model. *SOIL* 1: 399-410.
<https://doi.org/10.5194/soil-1-399-2015>
- Wagner, L.E. and Y. Yu. 1991. Digitization of profile meter photographs. *Trans. ASAE* 34(2): 412-416.
<https://doi.org/10.13031/2013.31677>
- Warner, W.S. 1995. Mapping a three-dimensional soil surface with hand-held 35 mm photography. *Soil & Tillage Research* 34(3): 187-197.
[https://doi.org/10.1016/0167-1987\(95\)00462-2](https://doi.org/10.1016/0167-1987(95)00462-2)
- Welch, R., T. Jordan, and A. Thomas. 1984. Photogrammetric technique for measuring soil erosion. *Journal of Soil and Water Conservation* 39(3): 191-194.
- WFI. 2009. Photogrammetry. Wikimedia Foundation, Inc. Available at:
<http://en.wikipedia.org/w/index.php?title=Photogrammetry&oldid=315599416>. Accessed 20 October 2009.
- Wilson, B. N., R. B. Leaf, and B. J. Hansen. 2001. Microrelief meter for field topography measurements. *Trans. ASABE* 44(2): 289-295.
<https://doi.org/10.13031/2013.4690>